Accepted Manuscript

Title: Synthesis of rhodamine based organic nanorods for efficient chemosensor probe for Al (III) ions and its biological applications

Authors: M. Maniyazagan, R. Mariadasse, M. Nachiappan, J. Jeyakanthan, N.K. Lokanath, S. Naveen, G. Sivaraman, P. Muthuraja, P. Manisankar, T. Stalin

Please cite this article as: M.Maniyazagan, R.Mariadasse, M.Nachiappan, J.Jeyakanthan, N.K.Lokanath, S.Naveen, G.Sivaraman, P.Muthuraja, P.Manisankar, T.Stalin, Synthesis of rhodamine based organic nanorods for efficient chemosensor probe for Al (III) ions and its biological applications, Sensors and Actuators B: Chemicalhttp://dx.doi.org/10.1016/j.snb.2017.07.106

Synthesis of rhodamine based organic nanorods for efficient chemosensor probe for Al (III) ions and its biological applications

M. Maniyazagan[a], R. Mariadasse[b], M. Nachiappan[b], J. Jeyakanthan[b], N. K. Lokanath[c],

S. Naveen[c], G. Sivaraman[d], P. Muthuraja[a], P. Manisankar[a], T. Stalin [a,e] *

a Department of Industrial Chemistry, School of Chemical Sciences, Alagappa University, Karaikudi-03, Tamil Nadu, India.

b Structural Biology and Bio-computing Lab, Department of Bioinformatics, Alagappa University, Karaikudi-04, Tamil Nadu, India.

c Dept. of Studies in Physics, University of Mysore, Mansagangotri, Mysore-06, India.

d Institute for Stem Cell Biology and Regenerative Medicine, Bangalore-560065, India.

e Department of Chemistry, University of Miami, Coral Gables, Miami, Florida 33124, United States

* Corresponding author E-mail address: drstalin76@gmail.com (Dr. T. Stalin)

*Dr. T. Stalin. Tel: +1(786)-381-5014.

Graphical Abstract
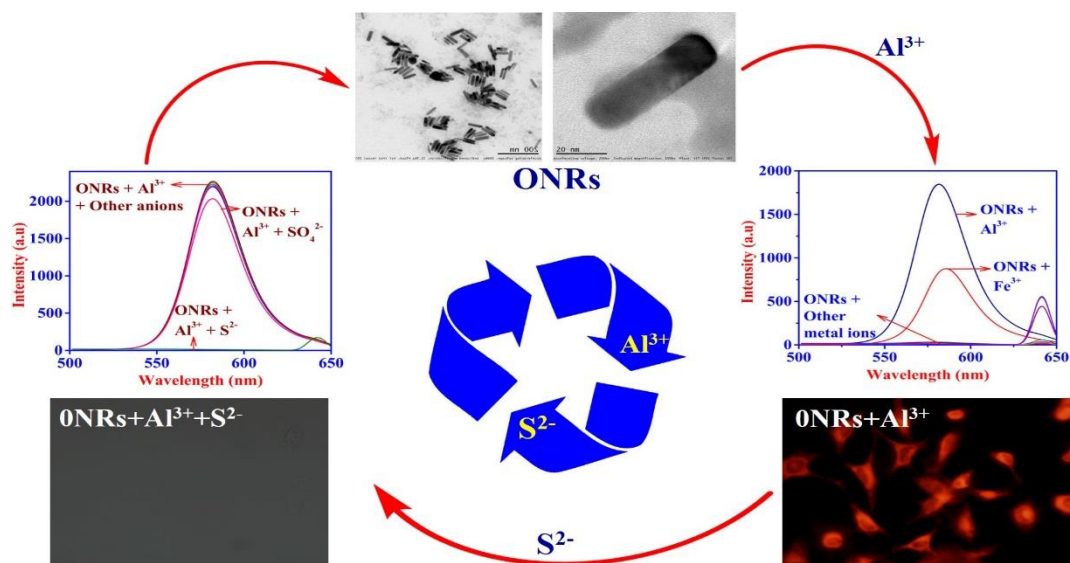
Highlights:

- A novel rhodamine-based organic nanorods (ONRs) was synthesized and characterized.

- The X-ray crystal structure analyses exhibit the spirolactam of rhodamine derivative RBD2.

- ONRs highly selective towards Al^{3+} ions over other metal ions.

- The 1:1 stoichiometric structure between ONRs and Al^{3+} ions were supported by Job's plot, Benesi-Hildebrand plot and DFT theoretical calculations.

- ONRs fluorescent sensor was used in imaging Al^{3+} ions in cultured HeLa cells.

Abstract

A novel highly selective rhodamine based organic nanorods (ONRs) was successfully designed and synthesised, which showed both absorption and fluorescence turn-on responses for Al^{3+} ions in aqueous solution. The ONRs possess strong fluorescence emission in aqueous solution. These spectral changes are sufficient to detection of Al^{3+} ions in the visible region of the spectrum and thus support naked eye detection. The aforesaid studies reveal that ONRs−Al^{3+} complex is highly selective and fully reversible in presence of sulphide anions. This study raises the new possibility of a highly selective and sensitive ONRs having multifunctional detection, including cation and anions, using a successive fluorescence response strategy in biological systems. Besides, the fluorescence microscopic studies confirmed that the fluorescent probe ONRs could be used as an imaging probe for detection of uptake of Al^{3+} ions in HeLa cells.

1. Introduction

Nanorods with shape anisotropy have received much attention due to their promising applications in chemical sensors, imaging, biomedicine, electronics and catalysis [1-8]. Reprecipitation was first introduced by Nakanishi and co-workers as a facile method to prepared organic nanomaterials, more and strategies have been developed for constructing organic nanomaterials with different morphologies. This organic nanomaterial better performances such as multicolour emission, chemiluminescence, chemical sensor, etc., [9-13].

Detection of various trivalent metal cations (M^{3+}) is a significant task for chemists since many M^{3+} ions play important roles in the environment and human daily physiological activity [14]. Trivalent chromium, Cr^{3+} is one of the most significant heavy metal elements. Currently interest on Cr^{3+} as an environmental pollutant has been increasing due to its build up to toxic

levels in the environment as a result of various agricultural and industrial activities [15, 16]. The United States Environmental Protection Agency (USEPA) has also considered this trivalent chromium species as a mutagenic and carcinogenic agent. Besides, Cr^{3+} is an essential nutrient for humans and it plays an important role in several biochemical processes at the cellular level. The defect of trivalent chromium ion in the human body would lead to different types of diseases, including diabetes and cardiovascular disease [17]. While excessive consumption of trivalent chromium ion (Cr^{3+}) can bind to DNA, it can negatively affect cellular structures and damage the cellular components [18, 19]. Remarkably, there is a greater need to develop an analytical method which can detect the presence of trivalent chromium ion (Cr^{3+}) in environmental and biological samples.

Iron, an essential trace element for both plants and animals, plays a significant role in enzyme catalysis [20], cellular metabolism [21] and as an oxygen carrier in hemoglobin and a cofactor in many enzymatic reactions. Consequently, Fe^{3+} deficiency leads to liver and kidney damages, anemia, heart diseases and diabetes [22]. Analytical techniques like atomic absorption spectroscopy [23], colorimetry [24], spectrophotometry [25] and voltammetry [26] have been used for both qualitative and quantitative detection of Fe^{3+} ions. But these techniques require sophisticated equipment's, tedious sample preparation procedures, and trained analysts.

Aluminum is the third highest abundant metallic element in the earth's crust. The amount of free Al^{3+} ions in the water is raised by leaching from soil due to acid rain. It is toxic to plants and kills aquatic animals in acidified water [27-30]. The World Health Organization (WHO) suggested the average daily human intake of Al^{3+} ions of around 3–10 mg and the weekly acceptable dietary intake of 7 mg/kg [31, 32]. The extensive use of Al^{3+} ions around us in the modern society are in water purification plants, food industry, pharmaceutical industries. The Al^{3+} ions toxicity causes microcytic hypochromic anaemia (chlorosis), Aluminum-related bone disease (ARBD),

encephalopathy and neuronal disorder leading to dementia, similarly its affects the absorption of iron in blood, leads to anaemia. Besides, the toxicity of aluminum causes its affects the central nervous system (CNS), is suspected to be complicated in neurodegenerative diseases such as Alzheimer's and Parkinson's diseases [33-37]. In the environment, the selective and sensitivity detection of Al^{3+} ions have significant importance for human health. Up to now, a number of fluorescent probes for Al^{3+} ions have been reported [38-43]. However, these probes might encounter some problems, such as poor water solubility and short wavelength. Therefore, there is still need to further develop water-soluble, highly selective and sensitive fluorescent probes for Al^{3+} ions. The rhodamine moiety has been used extensively in the field of chemosensors, particularly as a fluorescence chemodosimeter, given its fluorescence OFF–ON behaviour resulting from its unique structural design and properties. In this paper, for the first time, we report a facile approach to synthesis rhodamine based organic nanorods with controlled size using hydrothermal method. The ONRs can serve as a fluorescent probe for rapid, sensitive and selective detection of Al^{3+} ions in aqueous solution.

2. Experimental section

2.1. General Information and Materials

All of the materials for synthesis were purchased from commercial suppliers and used without further purification. The absorption spectra were recorded on a Schimadzu UV-PC-2401 UV-vis spectrophotometer using 10 mm path length quartz cuvettes in the range 300−800 nm wavelengths, while the fluorescence measurements were carried on a JASCO FP-8200 spectrofluorometer using 10 mm path length quartz cuvettes with a slit width of 5 nm at 298 K. The mass spectra of RBD2 using Agilent Technologies 6520 Accurate mass spectrometer. NMR spectra were recorded on a Varian FT-400 MHz instrument. The chemical shifts were recorded in parts per million (ppm) on the scale. The following abbreviations are used to

describe spin multiplicities in ^{1}H NMR spectra: s = singlet; d = doublet; t = triplet; m = multiplet. The transmission electron microscopy (TEM) images of the nanoparticles were recorded using a FEI Tecnai G2 S-TWIN High-Resolution Transmission Electron Microscope (HR-TEM) equipped with a LaB6 filament and operated at 200 KeV. The TEM specimens were prepared by dispersing the nanorods in ethanol and placing a drop of the dispersion on a Cu TEM grid covered with a holey carbon film, which was then dried.

2.2. Synthesis of the Rhodamine B hydrazide

In 100 ml flask, rhodamine B (1.20g, 2.5 mmol) was dissolved in 30 ml of ethanol, 3.0 ml of excess hydrazide hydrate (85%) was then added dropwise with vigorous stirring at room temperature. After the adding, the stirred mixture was heated to reflux in an air bath for 2 h. The solution changed from dark purple to light orange and became clear. Then the mixture was cooled and the solvent was removed under reduced pressure. 1M HCl (about 50 ml) was added to the solid in the flasks to generate a clear red solution. After that 1M NaOH (about 70 ml) was added slowly with stirring until the pH of the solution reached 9-10. The resulting precipitate was filtered and washed 3 times with 15 ml of water.

Yield: 85%, mp (°C): 191±2, ^{1}H-NMR (CDCl$_3$), δ (ppm): 1.16 (t, 12H, NCH$_2$CH$_3$, J = 7.0 Hz), 3.33 (q, 8H, NCH$_2$CH$_3$, J = 7.0 Hz), 3.64 (bs, 2H, NH$_2$), 6.32 (dd, 2H, Xanthene-H, J$_1$ = 9.0 Hz, J$_2$ = 2.4 Hz), 6.39(d, 2H, Xanthene-H, J = 2.4 Hz), 6.46 (d, 2H, Xanthene-H, J = 9.0 Hz), 7.11 (dd, 1H, Ar-H, J$_1$ = 5.4 Hz, J$_2$ = 3.3 Hz), 7.42 (d, 1H, Ar-H, J = 3.3 Hz), 7.44 (d, 1H, Ar-H, J = 3.3 Hz), 7.94 (dd, 1H, Ar-H, J$_1$ = 5.4 Hz, J$_2$ = 3.3 Hz). ^{13}C-NMR (CDCl$_3$) δ (ppm): 12.8, 44.58, 66.11, 76.81, 77.23, 77.44, 77.66, 98.23, 104.83, 108.28, 123.19, 124.03, 128.28, 130.24, 132.70, 149.11, 151.75, 154.06 and 166.35. FT-IR spectra of rhodamine b hydrazide revealed that the peak at 1735 cm^{-1}, the characteristic frequency for the C=O$_{Amide}$ bond of the rhodamine unit. Strong stretching frequencies at 3500 and 1690 cm^{-1} were observed in the IR spectra of rhodamine B hydrazide due to N–H stretching of NH$_2$ (primary amine) and

1 N-C=O (amide) stretching respectively. FT-IR (KBr) cm^{-1}: 3280, 3204 (νNH and νNH$_2$);

2 2923.38, 2810 (νCH); 1685.90 (νC=O); 1613.64, 1513.57 and 1496 (νAr=CH). ESI-Mass m/z

3 calculated value for 457.1; experimental value is 457.2

4 *2.3. Synthesis of the Rhodamine derivative (RBD2)*

5 Rhodamine-B hydrazide (0.46g, 1mmol) was dissolved in 20 ml absolute ethanol. An

6 excessive 4-bromo-2-thiophenecarboxaldehyde (4mmol) was added, and then mixture was

7 refluxed in an air bath for 6 h. After that, the solution was cooled (concentrated to 10 ml) and

8 allowed to stand at room temperature overnight. The precipitate which appeared next day was

9 filtered and washed 3 times with 10 ml absolute ethanol. After drying under reduced pressure

10 the reaction afforded 0.43g of RBD2 (76%) as pink solid, mp (°C): 217±2. ^{1}H NMR [CDCl$_3$],

11 SiMe$_4$, J (Hz), δ (ppm)]: ^{1}H-NMR (CDCl$_3$), δ (ppm): 1.13 (t, 12H, NCH$_2$CH$_3$, J = 7.1 Hz),

12 3.34 (q, 8H, NCH$_2$CH$_3$, J= 7.1 Hz), 6.29 (dd, 2H, Xanthene-H, J$_1$ = 8.9 Hz, J$_2$ = 2.2 Hz), 6.49

13 (d, 2H, Xanthene-H, J = 2.2 Hz), 6.53 (d, 2H, Xanthene-H, J = 8.9 Hz), 6.79 (dd, 1H, Phen-H),

14 6.86 (d, 1H, Phen-H), 7.09 (d, 1H, Phen-H), 7.16 (dd, 1H, Phen-H), 7.22 (d, 1H, Ar-H), 7.53

15 (m, 2H, Ar-H), 7.98 (d, 1H, Ar-H), ^{13}C NMR [CDCl$_3$, SiMe$_4$, δ(ppm)]: 164.94, 153.52, 151.52,

16 149.22, 142.52, 140.31, 133.65, 131.16, 129.16, 128.60, 128.12, 124.95, 124.17, 123.58,

17 109.72, 108.20, 106.08, 98.16, 77.66, 77.23, 76.61, 66.49, 44.54, 31.78, 14.31, 12.82. ESI

18 mass: calculated value for [($C_{42}H_{41}N_4O_3$) H] (M + H) is 629.61, experimental value 631.1.

19 *2.4. Synthesis of Organic nanorods*

20 The rhodamine derivative (RBD2) was dissolved in acetonitrile and a small amount

21 from this solution was injected into deionized water (20 ml) was put onto a 50 ml Teflon coated

22 stainless steel autoclave and heated at 150ºC for 8 hours. After being cooled to room

23 temperature, the organic nanorods were characterized by TEM and EDX analysis.

24 *2.5. Computational Details*

1   All ground-state optimizations were carried out by DFT [44] calculations using

2   Gaussian 09 [45]. All geometry optimizations were performed in the gas phase using the

3   B3LYP functional. For C, H, N, and O the 6-31G* basis set was used, whereas for Al^{3+} atoms

4   the SDD effective core potential was used. Vibrational frequency calculations were done to

5   verify the nature of the stationary points.

6   *2.6. Cell Culture and Fluorescence imaging*

7   HeLa, human cervical cancer cell line was procured from National Centre for Cell

8   Sciences, Pune, India and cultured in DMEM (Himedia, India) containing 10% heat-inactivated

9   fetal bovine serum (FBS), 100 units/ml penicillin G, 100 mg/ml streptomycin (Himedia, India),

10   2 mM glutamine (Gibco, USA), 25 mM HEPES, and 2 mM sodium bicarbonate under standard

11   conditions in CO_2 incubator (Eppendorf - New Brunswick Galaxy incubator). 90% confluent

12   cells were harvested and used for bioimaging studies.

13   HeLa cells were seeded in 6-well plates containing sterile circular cover-slips at a

14   density of 3×10^5 cells/well. After 8 h, experimental cells were incubated with 20 µl of ONRs

15   for 1h. After the incubation period, 20 µl the Al^{3+} were added and incubated for another 4h.

16   After the treatment period, the experimental cells were rinsed with PBS to remove the

17   remaining ONRs and Al^{3+} ions and visualized for fluorescence under Nikon Eclipse

18   fluorescence microscope (Nikon, Inc., Melville, NY).

19   **3. Results and discussion**

20   RBD2 was synthesized by refluxing 4-bromo-2-thiophenecarboxaldehyde with

21   rhodamine B hydrazide, in 83−85% yield (Scheme 1). RBD2 is stable and has been

22   characterized by usual spectroscopic techniques such as FT-IR, ^{1}H and ^{13}C NMR spectroscopy,

23   and ESI-MS (Fig. S1-S7). Further, the structure of RBD2 has been ascertained by X-ray

24   diffraction analysis. Compound RBD2 crystallizes in the Monoclinic, P21/n space group

8

1 (CCDC No: 1454981) (Fig. 1a, 1b and Table S1). The cation recognition properties of the

2 receptors have been established by absorption, fluorescence spectral studies.

3 *3.1. Characterization of organic nanorods*

4 For the transmission electron microscopy (TEM) measurements, the rods in aqueous

5 solution were deposited on top of a copper grid. This ONRs structure is retained in the

6 nanorods, as can be seen from the transmission electron microscopy (TEM) image of a ONRs

7 (Fig. 1c) and its electron diffraction pattern (Fig. 2c, inset) [46]. The nature of ONRs was

8 analysed by TEM and EDX, showing that the rod shaped ONRs (60nm) were uniformly formed

9 (Fig. 2). In EDX analysis signals corresponding to C and O were observed conforming the

10 organic nature of the ONRs (Fig. S8).

11 *3.2. Absorption studies of ONRs in presence of Al^{3+}*

12 UV−vis absorption spectral studies for ONRs in aqueous solution it shows an

13 absorption maximum at 322 nm, which may possibly be attributed to intramolecular $\pi-\pi^*$

14 charge transfer (CT) transition (Fig. S9). The ONRs−Al^{3+} binding leads to ring opening of the

15 spirolactam form to xanthene form. This structural change of ONRs is exhibited in the

16 absorption and fluorescence spectral studies. Thus, the selectivity of ONRs was checked with

17 Na^+, Mg^{2+}, K^+, Ca^{2+}, Fe^{2+}, Co^{2+}, Ni^{2+}, Cu^{2+}, Fe^{3+}, Pb^{2+}, Pd^{2+} and Al^{3+} in aqueous solution. A

18 significant change in absorption spectra was observed only in presence of Al^{3+}. For other metal

19 ions, there is no significant colour change or change in the absorption spectrum was observed

20 (Fig. 3a). In the absorption titration spectra (0 equiv. to 2 equiv. of Al^{3+}), a new absorption

21 band appeared around 558 nm (Fig. 3b), and the solution turned from colourless to pink colour.

22 The measured detection limit was found to be 4.1 nM for Al^{3+}.

23 The visual colour change of the solution from colourless to deep magenta is a

24 consequence of the ONRs strong affinity with Al^{3+} ions in aqueous solution. The significant

25 change in absorption spectra could be attributed to the conjugation of the thiophene moiety of

ONRs with the binding site of the Al^{3+} (Scheme S1). The formation of the peak 558 nm is particularly due to the bond cleavage of the spirolactam ring structure of ONRs and successive formation of the xanthene form. The spectral changes due to formation of the ONRs–Al^{3+} complex. Upon gradual addition of Al^{3+} ions to ONRs in aqueous solution, a concomitant red shift in the spectral position at 558 nm was observed along with an increase in the absorption intensity. The emergence of the absorption band at 558 nm was due to the opening of the spirolactam ring of the rhodamine moiety along with a colour change from colourless to deep magenta (Fig. S12) [46]. Hence, the probable binding constant for the formation of ONRs–Al^{3+} complex is calculated on the basis of change in absorption maxima at 558 nm by considering a 1:1 binding stoichiometry. The possible binding constant (K) determined by the Benesi– Hildebrand method [47-51] was found to be 4.675×10^4 M^{-1} (Fig. S10). Job's plot analysis showed that the complex formed in solution state is a 1:1 ONRs:Al^{3+} stoichiometric reaction (Fig. S11).

3.3. Fluorescence studies of ONRs in presence of Al^{3+}

To evaluate the selectivity of the present sensing system, control experiments were performed [52]. The fluorescence selectivity study of ONRs with Al^{3+} ions and other metal ions was also studied in aqueous solution in the absence and presence of an excess of each of the metal ions (Fig. 4a). From Figure 3a, an excitation maximum of the ONRs at 322 nm wavelength did not show any significant change in fluorescence spectra over the range from 500 nm to 700 nm. These results showed the absence of Al^{3+} ions the probe ONRs remains in the spirolactam form. In addition of Al^{3+} ions to this ONRs, it's leads to a significant OFF–ON fluorescence response at 585 nm, with a naked eye detection of pink colour. OFF–ON responses for the emission maxima at 585 nm on binding to Al^{3+} ions, it's shows that the opening of the spirolactam ring in ONRs on metal ion coordination. It can also be conformed from Figure 4a that the ONRs−Al^{3+} binding induced ring-opening of ONRs and the formation

1   of xanthene moiety is highly selective toward Al^{3+} ions and does not show any significant

2   spectral changes for other metal ions (Na^+, Mg^{2+}, K^+, Ca^{2+}, Fe^{2+}, Co^{2+}, Ni^{2+}, Cu^{2+}, Fe^{3+}, Pb^{2+},

3   Pd^{2+} and Al^{3+}). The fluorescence titration spectra of the ONRs was enhanced with increasing

4   concentration of Al^{3+} ions. As represent in Figure 4b the fluorescence spectra of ONRs was

5   enhanced with increasing concentration of Al^{3+} ions, which also confirmed that the ONRs

6   shows a high sensitivity towards Al^{3+} ion. The results indicated that the spirolactam ring was

7   opened and conjugated structure was formed. The recognition interaction was completed

8   immediately after the addition of Al^{3+} within 1 min, and hence, ONRs could be used in real-

9   time determination of Al^{3+} in environmental and biological conditions. There was a significant

10   emission intensity enhancement with Al^{3+} which indicates that compound ONRs is an excellent

11   turn-on sensor for Al^{3+} [53]. The binding affinity of Al^{3+} ions induces opening of the

12   spirolactam ring in ONRs with an associated switch on UV−vis absorption spectra in the range

13   500 nm − 580 nm, which has a spectral overlap with the emission spectrum of the thiophene

14   moiety. These results suggest that the plausible route for non–radiative transfer of excitation

15   energy between donor thiophene moiety to acceptor xanthene moiety and induces an

16   intramolecular FRET process. In the fluorescent probe ONRs alone the FRET pathway is

17   totally suppressed, and only fluorescence emission maxima near 480 nm is observed when

18   excited at 322 nm. Binding of the ONRs to Al^{3+} ions induces the FRET process to produce an

19   intense red emission. When ONRs titrated with increasing concentration of Al^{3+} ions the

20   emission band exhibit with a λ_{max} at 457 nm starts to decrease along with a concurrent

21   formation of a new fluorescence maxima at 585 nm. The above changes in fluorescence spectra

22   was also conformed via naked eye detection, and the colour changed to reddish-pink (Fig. S12).

23   *3.4. DFT Studies*

24   The mode of binding of Al^{3+} ions with the ONRs was also studied by DFT calculations.

25   The stoichiometry of the complexes was found to be 1:1 on the basis of absorption, emission

1 studies and these mononuclear complexes was modelled by DFT calculations. The geometry

2 optimization for free ONRs and the corresponding complex was done by DFT calculations. For

3 metal complex, ground-state-optimized structure of free ONRs were generated and Al^{3+} ions

4 were kept well in the core of the amide O and imine N as donor atoms at a noninteracting

5 distance.

6 The HOMO−LUMO orbital energies and spatial distributions for ONRs and ONRs-

7 Al^{3+} were also determined (Fig. 5). The energy gaps between the HOMOs and LUMOs for

8 receptor ONRs were 172.24 kcal mol^{-1}. Similarly, for complex [ONRs-Al^{3+}] the energy gaps

9 were found to be 23.33 kcal mol^{-1} (Table S2). These results suggest that the binding mode of

10 Al^{3+} ions adopts S-N-O co-ordination by bonding through the one sulphur atom of the

11 thiophene group, one nitrogen of the imine group and one oxygen atom of the carbonyl group,

12 resulting in a nearly planar geometry around Al^{3+} ions. The optimized structures of Al^{3+} ions

13 with receptors ONRs show that the individual low-energy complexation occurs between Al^{3+}

14 ions and S-N-O atoms of the free ONRs. Hence, the interaction of S, N and O with Al^{3+} ions

15 could change the HOMO−LUMO energy levels and the electronic transitions. It should happen

16 between the rhodamine-centered HOMOs and the π*-type LUMOs, located in the rhodamine

17 unit. Furthermore, the DFT studies showed that the energy gap between the HOMO−LUMO

18 of the complex becomes smaller than complexation, which correlates with the observed red

19 shift in the absorption spectra.

20 *3.5. Absorption studies of ONRs−Al^{3+} complex in presence of S^{2-}*

21 We have further studied the impact of different anions on the cleavage of this

22 ONRs−Al^{3+} complex and their effect on the reversibility of this complex to regenerate ONRs.

23 The absorption properties of the ONRs−Al^{3+} complex was studied in presence of different

24 anions such as F^-, Cl^-, Br^-, I^-, CN^-, $H_2PO_4^-$, NO_3^-, ClO_3^-, ClO_4^-, HSO_3^-, SO_4^{2-}, PO_4^{3-}, and

25 S^{2-}. The absorption spectral studies suggest that the regeneration of compound ONRs is

1   observed only by adding S^{2-} to the solution having ONRs−Al^{3+}, whereas other anions did not

2   show any remarkable changes in absorption spectra (Fig. 6a). The absorption spectral studies

3   of the titration experiment (Fig. 3b) was similar but in reverse direction to the spectra obtained

4   with Al^{3+} (Fig. 6b). This fact is evidence that ONRs is recovered from ONRs−Al^{3+} in presence

5   of S^{2-}.

6   *3.6. Fluorescence studies of ONRs−Al^{3+} complex in presence of S^{2-}*

7   In another control experiment [52], the fluorescence spectral studies also show that the

8   emission spectra of the ONRs−Al^{3+} complex returns to its original ONRs state, selectively in

9   presence of S^{2-} ions (Fig. 7a). In addition, the fluorescence "ON−OFF'' switching property of

10   the fluorescent complex ONRs–A^{3+}, we have studied in fluorescence titration experiment.

11   Fluorescence titration experiment (Fig. 7b) shows that the intensity of the fluorescence

12   emission maxima decreases with increasing concentration of S^{2-} ions and on addition of S^{2-}

13   anion both the intensity and the fluorescence spectrum closely match those of ONRs (Fig. 7b).

14   The aforesaid results suggested that the ONRs was recycled during the detection of S^{2-} ions.

15   The ONRs–Al^{3+} spectral binding studies it was conform that the binding induced

16   breakage of the spirolactam ring of ONRs initiates the FRET pathway for efficient transfer of

17   energy from thiophene moiety to the xanthene moiety. It is evident that the regeneration of

18   ONRs from ONRs–Al^{3+} complex is possible in presence of S^{2-} ion then the removal of Al^{3+}

19   disturb the FRET process. Thus, increasing concentration of S^{2-} ions to the ONRs–Al^{3+}

20   complex in fluorescence emission spectrum (Fig. 7b) which is equivalent to the fluorescence

21   spectra of ONRs (when excited at 322 nm). The aforesaid fact suggests strong evidence of the

22   dissociation of ONRs-Al^{3+} complex in presence of S^{2-} anions to restore the original structure

23   of ONRs. The sensing mechanism of ONRs and ONRs−Al^{3+} complex was further studied in

24   presence of other ions, which may interfere in estimation of Al^{3+} and S^{2-} (Fig. S13). The ONRs

1   and the ONRs−Al^{3+} complex both performed well in presence of other ions and sensed the

2   corresponding analytes from a competitive experiment studies.

3   *3.7. Fluorescence lifetime studies*

4   Additionally, time dependent photoluminescence decay process had been carried out

5   for the life time measurement of ONRs and ONRs-Al^{3+} complex. A pinch of milk powder had

6   been used to prompt the instrument. The proposed mechanism was also well propped up by the

7   fluorescence data. In the fluorescence lifetime decay experiment (λ_{em} = 585 nm), the average

8   luminescence lifetime of ONRs was found to be 0.26 ns at which 455 nm nano LED source

9   was used. After the addition of Al^{3+} ions to the solution of ONRs, the average luminescence

10   lifetime (λ_{emi} = 585 nm) of ONRs-Al^{3+} system increased to 2.38 ns. In both the cases, the

11   fluorescence decay curve was fitted to double-exponential decay theoretical calculation. From

12   the obtained results, there is a delay (2.12 ns) in the decay process when Al^{3+} ions interact with

13   the ONRs; hence it is proved that there is a platform for the enhanced fluorescence in the case

14   ONRs-Al^{3+} interaction (Fig. 8).

15   *3.8. Biological Studies of ONRs in the Presence of Al^{3+}*

16   The binding properties of ONRs with Al^{3+} ions and exciting photophysical properties,

17   such as high sensitivity, selectivity, and fast response, we studied their potential use in

18   fluorescence imaging of the Al^{3+} ions in living cells. The ability of ONRs to detect intracellular

19   Al^{3+} ions in HeLa cells was evaluated by fluorescence imaging studies (Fig. 9). The HeLa cells

20   incubated for 2 h at 37 °C with ONRs showed no fluorescence. However, the addition of Al^{3+}

21   ions (10 μM) to the preincubated cells (for 2 h) exhibited the enhanced red fluorescence

22   intensity. These results suggested that ONRs was cell permeable and an effective intracellular

23   Al^{3+} ions with "off-on" red colour fluorescence emission.

24   **4. Conclusion**

1   Rhodamine based organic nanorods with controlled size were successfully synthesized

2   by hydrothermal method. This ONRs could be used as a fast, fluorescence sensor for Al^{3+} and

3   S^{2-} ions in aqueous solution. The visible changes the FRET based fluorescence response makes

4   it a dual probe for naked eye detection through change in colour and fluorescence spectroscopy.

5   The complex formed between ONRs and Al^{3+} ions is dissociable only in presence of S^{2-} ions,

6   which makes the ONRs$-Al^{3+}$ complex an efficient sensor for S^{2-} ions. From the extensive

7   spectroscopic studies, it is clear that the ONRs and ONRs$-Al^{3+}$ complex could be used as a

8   fluorescent sensor for the detection of Al^{3+} and S^{2-}ions. The ONRs shows intense change in its

9   fluorescence emission when bound to Al^{3+} ions in physiological conditions. Hence, the

10   capability of ONRs as a probe for intracellular detection of Al^{3+} ions by fluorescence

11   microscopy was also studied. Furthermore, we have demonstrated that the ONRs is applicable

12   for Al^{3+} ions imaging in the HeLa cells.

13   **ASSOCIATED CONTENT**

14   * Supporting Information

15   Crystallographic data in CIF format for compound 4E (RBD2) have been deposited at

16   the Cambridge Crystallographic Data Centre, CCDC No. 1454981. Copies of CIF are available

17   free of charge from The Director, CCDC, 12 Union Road, Cambridge, CB2 1EZ, UK (Fax:

18   +44 1223 336 033; email: deposit@ccdc.cam.ac.uk or http://www.ccdc.cam.ac.uk). Selected

19   bond angles and bond lengths of ONRs. ^{1}H, ^{13}C, and ESI-Mass data of rhodamine B hydrazide

20   and ONRs, single-crystal data of ONRs. Job's plot for the absorption titration of ONRs with

21   Al^{3+}; B$-$H plot of ONRs binding with Al^{3+} ions.

22   **AUTHOR INFORMATION**

23   Corresponding Author

24   *Dr. T. Stalin. Tel: +1(786)-381-5014

25   E-Mail: drstalin76@gmail.com.

1 **Notes**

2 The authors declare that there is no competing financial interest.

3 **ACKNOWLEDGMENTS**

11

12

13

14

REFERENCES

[1] Y. Huang, X. Duan, Q. Wei and C.M. Lieber, Science. 291 (2001) 630.

[2] R. Costi, A.E. Saunders and U. Banin, Angew. Chem., Int. Ed. 49 (2010) 4878.

[3] J.A. Dahl, B.L.S. Maddux and J.E. Hutchison, Chem. Rev. 107 (2007) 2228.

[4] H. Fan, Y. Lu, A. Stump, S.T. Reed, T. Baer, R. Schunk, V. Perez-Luna, G.P. Lopez and C.J. Brinker, Nature. 405 (2000) 56.

[5] P.C. Ray, Chem. Rev. 110 (2010) 5332.

[6] X. Chen, S. Shen, L. Guo and S.S. Mao, Chem. Rev. 110 (2010) 6503.

[7] A.I. Hochbaum and P. Yang, Chem. Rev. 110 (2009) 527.

[8] Q. Liu, Z. Yan, N.L. Henderson, J.C. Bauer, D.W. Goodman, J.D. Batteas and R.E. Schaak, J. Am. Chem. Soc. 131 (2009) 5720.

[9] J. Yang, L.L. Chng, X. Yang, X. Chen and J.Y. Ying, Chem. Commun. 50 (2014) 1141.

[10] H. Kasai, H.S. Nalwa, H. Oikawa, S. Okada, H. Matsuda, N. Minami, A. Kakuta, K. Ono, A. Mukoh and H. Nakanishi, Jpn. J. Appl. Phys. 31 (1992) 1132.

[11] X.J. Zhang, G.D. Yuan, Q.S. Li, B. Wang, X.H. Zhang, R.Q. Zhang, J.C. Chang, C.S. Lee and S.T. Lee, Chem. Mater. 20 (2008) 6945.

[12] H. Bi, H.Y. Zhang, Y. Zhang, H.Z. Gao, Z.M. Su and Y. Wang, Adv. Mater. 22 (2010) 1631–1634.

[13] J.C. Xiao, Z.Y. Yin, H. Li, Q. Zhang, F. Boey, H. Zhang and Q.C. Zhang, J. Am. Chem. Soc. 132 (2010) 6926.

[14] (a) L. Prodi, F. Balletta, M. Mantalti and N. Zaccheroni, Coord. Chem. Rev. 205 (2000) 205, (b) Q. Zhao, F. Li and C. Huang, Chem. Soc. Rev. 39 (2010) 3007.

[15] S. Saha, P. Mahato, U. Reddy G, E. Suresh, A. Chakrabarty, M. Baidya, Sudip K. Ghosh, and A. Das, Inorg. Chem., 51 (2012) 336.

[16] A.M. Zayed, N. Terry, Plant and Soil, 249 (2003) 139-156.

[17] A.K. Singh, V.K. Gupta, B. Gupta, Analytica Chimica Acta, 585 (2007) 171-178.

[18] H. Arakawa, R. Ahmad, M. Naoui, H.-A. Tajmir-Riahi, The Journal of Biological Chemistry, 275 (2000) 10150-10153.

[19] H. Arakawa, F. Wu, M. Costa, W. Rom, M. Tang, Carcinogenesis, 27 (2006) 639-645.

[20] Z.Q. Yan, S.Y. Guang, H.Y. Xu, X.Y. Liu, Analyst, 136 (2011) 1916–1921.

[21] N.R. Chereddy, K. Suman, P.S. Korrapati, S. Thennarasu, A.B. Mandal, Dyes and Pigments, 95 (2012) 606.

[22] Brugnara C. Iron deficiency and erythropoiesis: new diagnostic approaches. Clin Chem, 49 (2003) 1573.

[23] C. Brugnara, Clinical Chemistry, 49 (2003) 1573.

[24] A. Ohashi, H. Ito, C. Kanai, H. Imura, K. Ohashi, Talanta, 65 (2005) 525.

[25] Z.-Q. Liang, C.-X. Wang, J.-X. Yang, H.-W. Gao, Y.-P. Tiang, X.-T. Tao, M.-H. Jiang, New Journal of Chemistry, 31 (2007) 906.

[26] S. Lunvongsa, M. Oshima and S. Motomizu, Talanta, 68 (2006) 969.

[27] (a) J. Sun, B. Ye, G. Xia, H. Wang, Sensors and Actuators B, 249 (2017) 386, (b). R.A. Yokel, Neurotoxicology, 21 (2000) 813.

[28] S. Chemate and N. Sekar, Sensors and Actuators B, 220 (2017) 1196.

[29] J. Ren, H. Tian, Sensors. 7 (2007) 3166.

[30] R.A. Yokel, Neurotoxicology. 21 (2000) 813.

[31] J. Barcelo, C. Poschenrieder, Environ. Exp. Bot. 48 (2002) 75.

[32] Z. Krejpcio, R.W. Wojciak, Pol. J. Environ. Stud. 11 (2002) 251.

[33] G.D. Fasman, Coord. Chem. Rev. 149 (1996) 125.

[34] P. Nayak, Environ. Res. 89 (2002) 111.

[35] C.S. Cronan, W.J. Walker, P.R. Bloom, Nature. 324 (1986) 140.

[36] G. Berthon, Coord. Chem. Rev. 228 (2002) 319.

[37] D.R. Burwen, S.M. Olsen, L.A. Bland, M.J. Arduino, M.H. Reid, W.R. Jarvis, Kidney Int. 48 (1995) 469.

[38] S. Goswami, K. Aich, S. Das, A.K. Das, D. Sarkar, S. Panja, T.K. Mondal and S.K. Mukhopadhyay, Chem. Commun. 49 (2013) 10739-10741.

[39] D. Maity and T. Govindaraju, Chem. Commun. 46 (2010) 4499–4501.

[40] D. Maity and T. Govindaraju, Chem. Commun. 48 (2012) 1039–1041.

[41] M. Arduini, F. Felluga, F. Mancin, P. Rossi, P. Tecilla, U. Tonellato and N. Valentinuzzib, Chem. Commun. 2003 1606-1607.

[42] Z. Chen, Y. Sun, L. Zhang, D. Sun, F. Liu, Q. Meng, R. Wang and D. Sun, Chem. Commun. 49 (2013) 11557-11559.

[43] T. Han, X. Feng, B. Tong, J. Shi, L. Chen, J. Zhic and Y. Dong, Chem. Commun. 48 (2012) 416–418.

[44] W. Koch, M.C. Holthausen, Wiley-VCH: Weinheim. 2000.

[45] (a) A.D. Becke, J. Chem. Phys. 98 (1993) 5648. (b) C. Lee, W. Yang, R.G. Parr, Phys. Rev. B. 37 (1988) 785. (c) A.D. Becke, Phys. Rev. A: At., Mol., Opt. Phys. 38 (1988) 3098.

[46] L. Fan, J-C. Qin, T-R. Li, B-D. Wang, Z-Y. Yang, Sensors and Actuators B, 203 (2014) 550.

[47] C. Zhang, Y. Yan, Y.S. Zhao and J. Yao, Annu. Rep. Prog. Chem., Sect. C: Phys. Chem. 109 (2013) 211.

[48] M. Maniyazagan, R. Mariadasse, J. Jeyakanthan, N.K. Lokanath, S. Naveen, K. Premkumar, P. Muthuraja, P. Manisankar, T. Stalin, Sensors and Actuators B, 238 (2017) 565.

[49] S. Mohandoss, M. Maniyazagan, T. Stalin, Mater. Sci. Eng. C. 48 (2015) 94.

1 [50] M. Maniyazagan, S. Mohandoss, K. Sivakumar, T. Stalin, Spectrochim. Acta Part A. 133

2   (2014) 73.

3 [51] M. Maniyazagan, C. Rameshwaran, R. Mariadasse, J. Jeyakanthan, K. Premkumar, T.

4   Stalin, Sensors and Actuators B, 242 (2017) 1227–1238.

5 [52] R. Zhang, W. Chen, Biosensors and Bioelectronics, 55 (2014) 83.

6 [53] J. Ni, Q. Li, B. Li, L. Zhang, Sensors and Actuators B, 186 (2013) 278.

7

8

9

10

11

12

13

14

15

16

17

18

19

20

21

22

23

24

25

26

27

28

29

1   **Scheme 1.** Synthetic Scheme for the fluorescent probe RBD2.

2

3   **Figure 1.** (a) X-ray crystal structure of RBD2 showing displacement ellipsoids drawn at the

4   30% probability level. Hydrogen atoms have been omitted for clarity. (b) The

5   crystal packing of RBD2. Intermolecular interactions have been omitted for clarity.

6   **Figure 2.** (a), (b) TEM, images of ONRs, (c) SAED pattern of the ONRs.

7   **Figure 3.** (a) UV−vis absorption spectra of ONRs observed upon addition of different metal

8   ions (Na^+, Mg^{2+}, K^+, Ca^{2+}, Fe^{2+}, Co^{2+}, Ni^{2+}, Cu^{2+}, Fe^{3+}, Pb^{2+}, Pd^{2+} and Al^{3+}) in

9   aqueous solution. (b) UV−vis titration spectra of ONRs upon addition of Al^{3+} in

10   aqueous solution (0 to 2 equiv.).

11   **Figure 4.** (a) Changes of the fluorescence emission of ONRs observed upon addition of metal

12   ions (Na^+, Mg^{2+}, K^+, Ca^{2+}, Fe^{2+}, Co^{2+}, Ni^{2+}, Cu^{2+}, Fe^{3+}, Pb^{2+}, Pd^{2+} and Al^{3+}) in

13   aqueous solution. (b) Fluorescence titration spectra of ONRs upon addition of 0 to 2

14   equiv. of Al^{3+} in aqueous solution (λ_{ex} = 322 nm).

15   **Figure 5.** Frontier molecular orbitals of receptors and their complex with the Al^{3+} ions. HOMO

16   and LUMO active representation of ONRs (a & b). HOMO and LUMO active

17   representation of ONRs-Al^{3+} (c & d).

18   **Figure 6.** (a) Changes in the absorption spectra of ONRs−Al^{3+} complex in presence of different

19   anions. (b) UV−vis titration spectra of ONRs with 2 equiv. of Al^{3+} upon addition of

20   sodium sulfide (30 μM) in aqueous solution.

21   **Figure 7.** (a) Changes in the fluorescence spectra of ONRs−Al^{3+} complex in presence of

22   different anions. (b) Fluorescence titration spectra of ONRs with 2 equiv. of Al^{3+}

23   upon addition of sodium sulfide (30 μM) in aqueous solution.

24   **Figure 8.** Lifetime measurement studies of ONRs (a) and ONRs–Al^{3+} (b).

1 **Figure 9.** The fluorescence microscope images of HeLa cells with absence of metal ions ONRs

2 (a), Al^{3+} (b) did not show any fluorescence and ONRs-Al^{3+} (c) showed intense red

3 fluorescence.

4

5

6

7

8

9

10

11

12

13

14

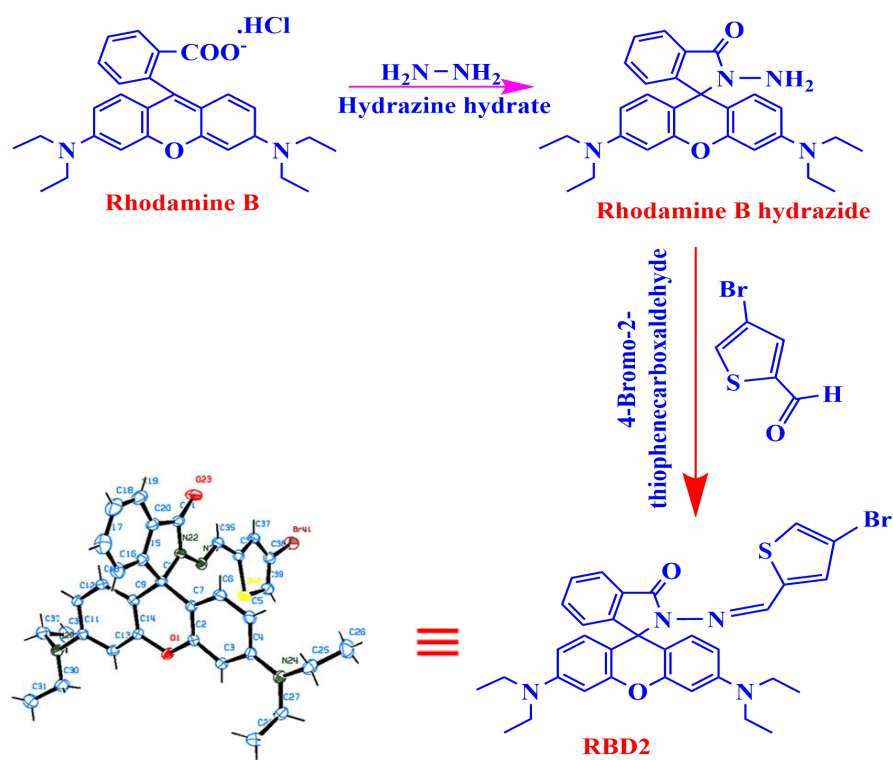15

16

17

18

19

20

21

22

23

24

25

26

27

28

29

1

2

3

4

5

6

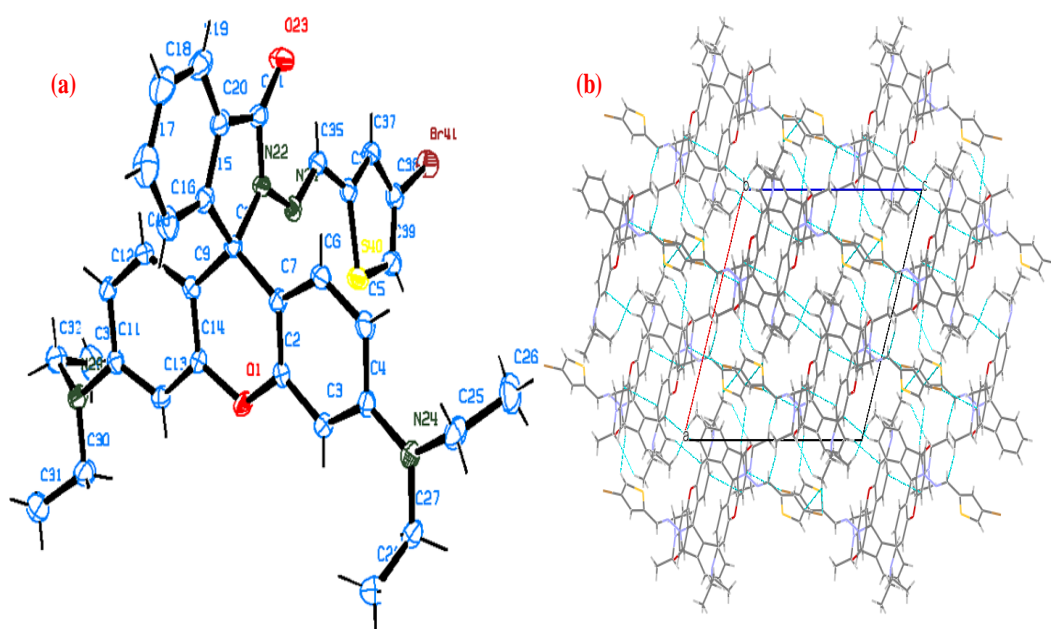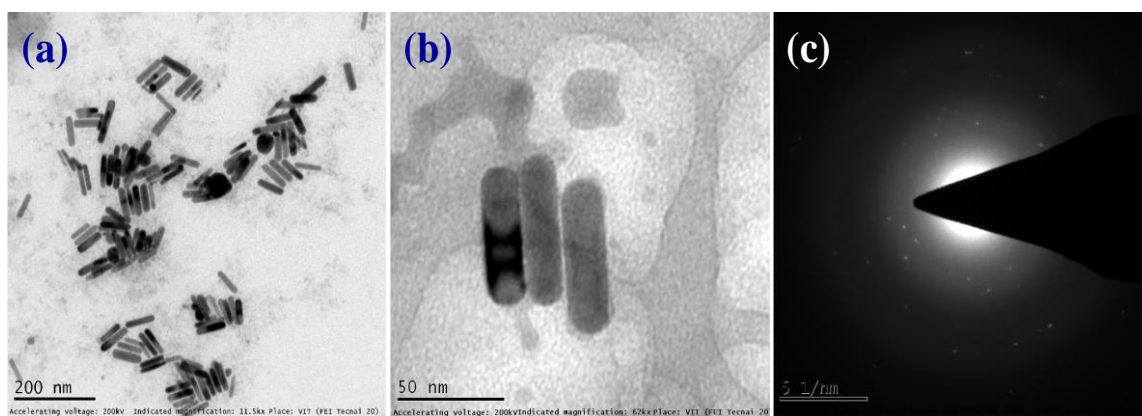7 **Scheme 1.** Synthetic Scheme for the fluorescent probe RBD2.

8

1

2

3

4

5

6

7

8

9

10

11

12

13

14

15 **Figure 1.** (a) X-ray crystal structure of RBD2 showing displacement ellipsoids drawn at the

16   30% probability level. Hydrogen atoms have been omitted for clarity. (b) The crystal

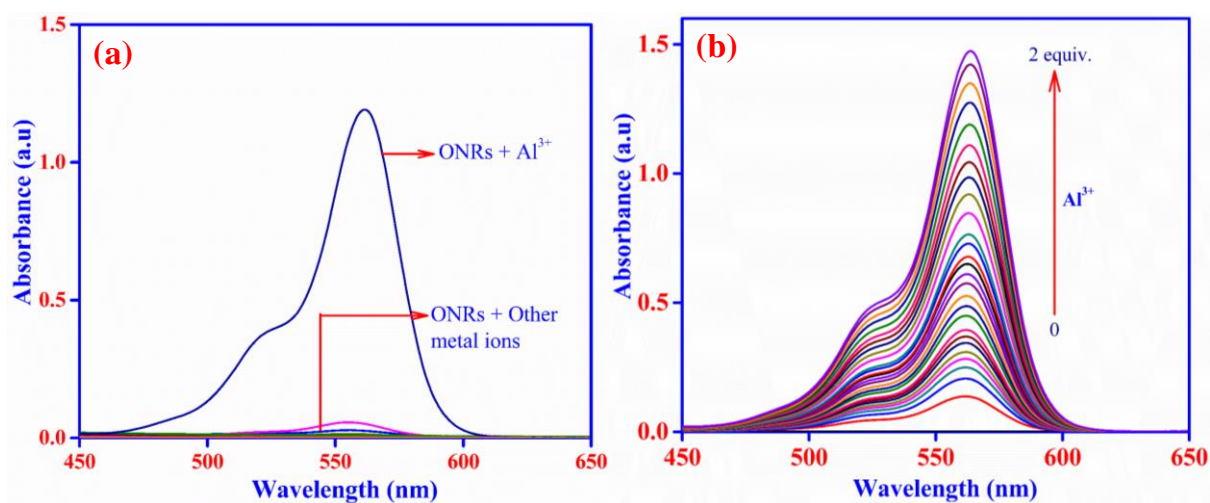17   packing of RBD2. Intermolecular interactions have been omitted for clarity.

1

2

3

4

5

6

7

8

9

10

11

12

13

14

15 **Figure 2.** (a), (b) TEM, images of ONRs, (c) SAED pattern of the ONRs.
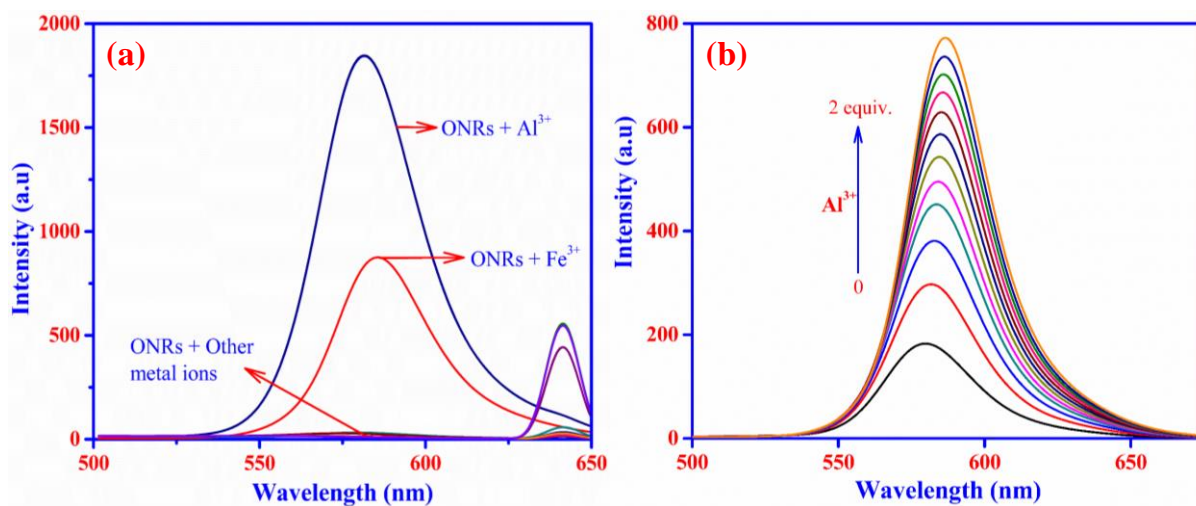
16

17

18

19

20

21

22

23

24

25

1

2

3

4

5

6

7

8

9

10

11

Figure 3. (a) UV−vis absorption spectra of ONRs observed upon addition of different metal ions (Na$^+$, Mg^{2+}, K$^+$, Ca^{2+}, Fe^{2+}, Co^{2+}, Ni^{2+}, Cu^{2+}, Fe^{3+}, Pb^{2+}, Pd^{2+} and Al^{3+}) in aqueous solution. (b) UV−vis titration spectra of ONRs upon addition of Al^{3+} in aqueous solution (0 to 2 equiv.).
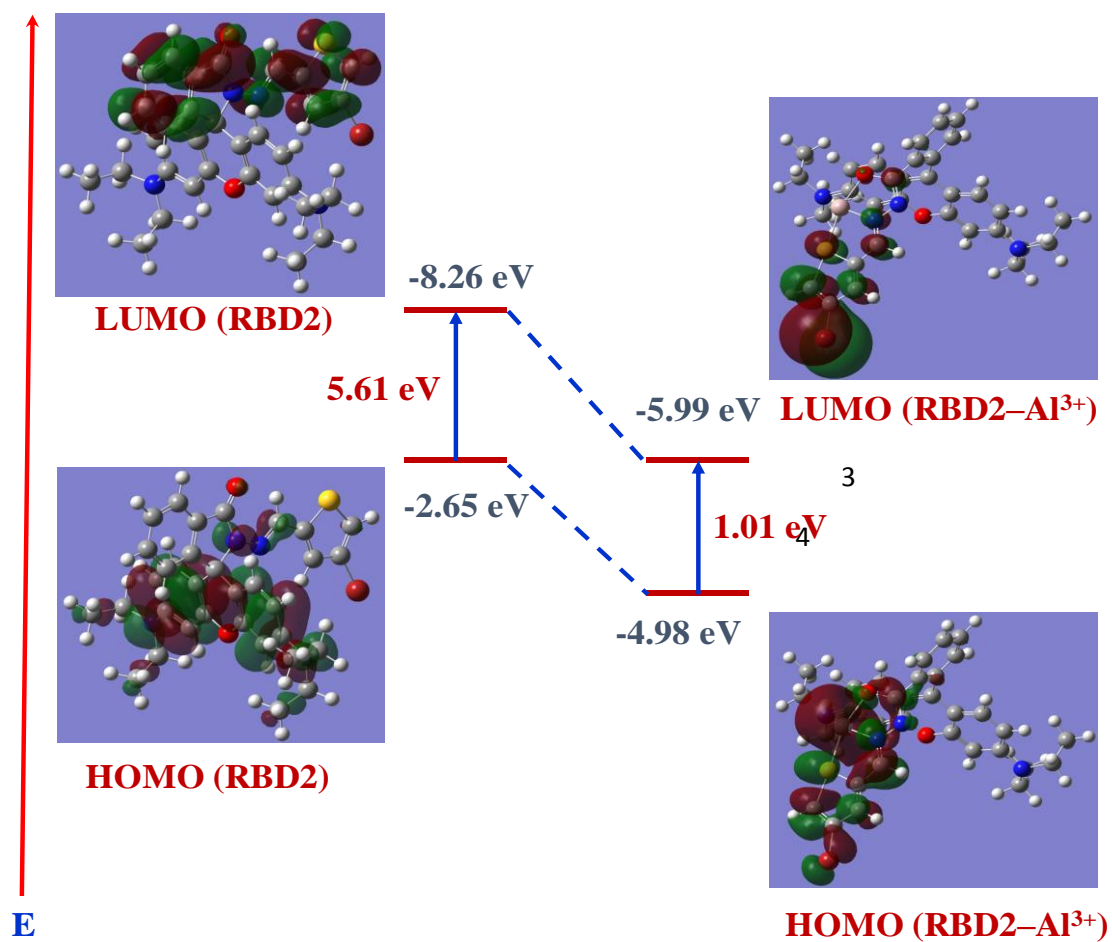
16

17

18

19

20

21

1

2

3

4

5

6

7

8

9

10

11

12

13

14 **Figure 4.** (a) Changes of the fluorescence emission of ONRs observed upon addition of metal

15 ions (Na$^+$, Mg^{2+}, K$^+$, Ca^{2+}, Fe^{2+}, Co^{2+}, Ni^{2+}, Cu^{2+}, Fe^{3+}, Pb^{2+}, Pd^{2+} and Al^{3+}) in

16 aqueous solution. (b) Fluorescence titration spectra of ONRs upon addition of 0 to 2

17 equiv. of Al^{3+} in aqueous solution (λ_{ex} = 322 nm).

18

19

20

1

LUMO (RBD2)

-8.26 eV

5.61 eV

-2.65 eV

HOMO (RBD2)

E

-5.99 eV **LUMO (RBD2–Al³⁺)**

3

1.01 eV

-4.98 eV

HOMO (RBD2–Al³⁺)

5

6
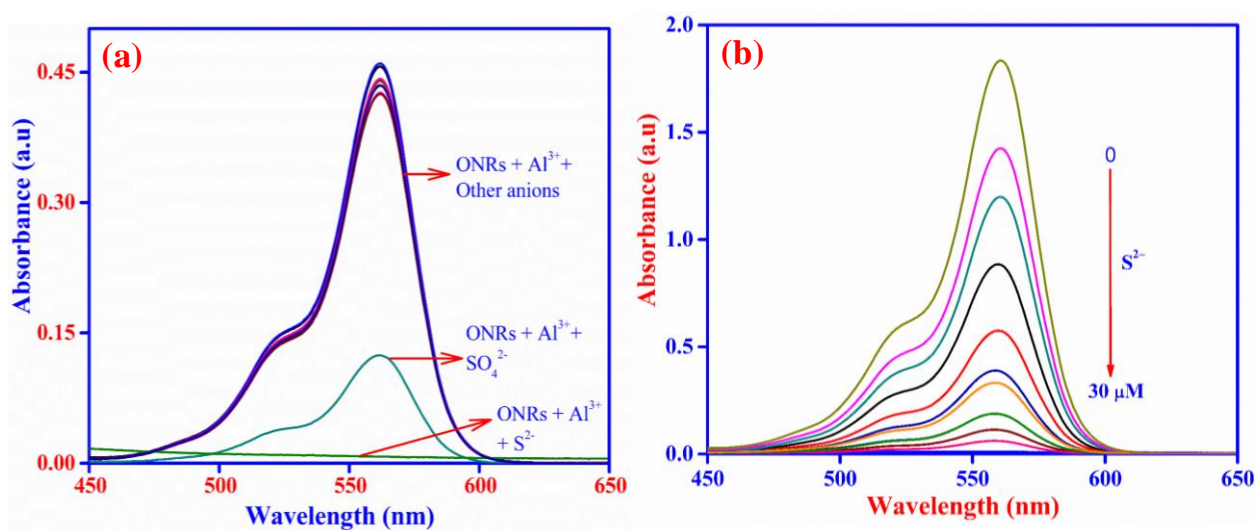
7

8

9

10

11

12

13

14

15

16

17

18

1 **Figure 5.** Frontier molecular orbitals of receptors and their complex with the Al^{3+} ions. HOMO

2 and LUMO active representation of ONRs (a & b). HOMO and LUMO active
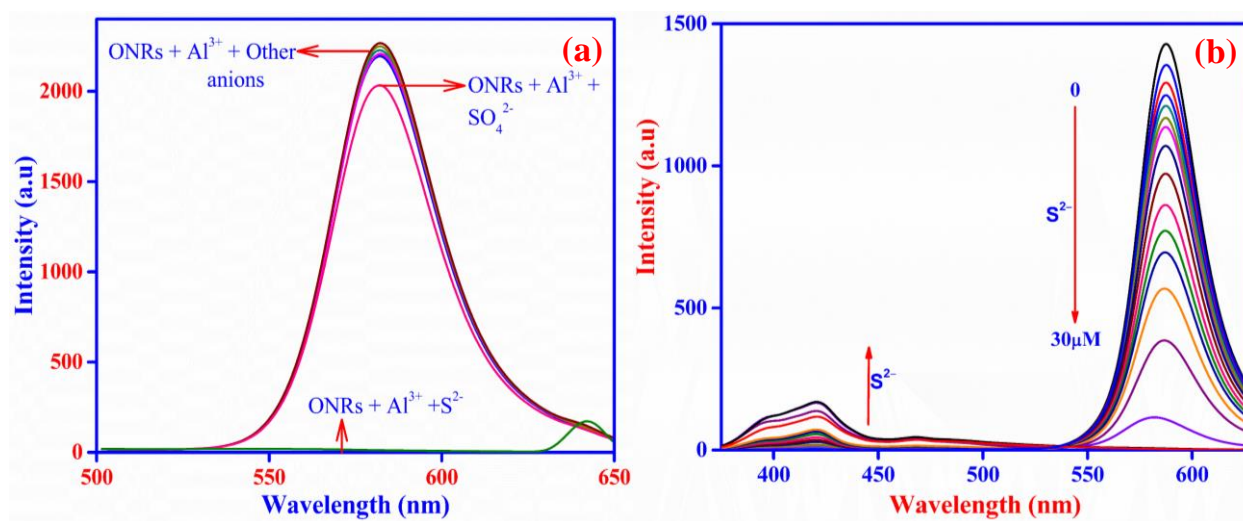
3 representation of ONRs-Al^{3+} (c & d).

4

5

6

7

8

9

10

11

12

13

14

15

16 **Figure 6.** (a) Changes in the absorption spectra of ONRs−Al^{3+} complex in presence of different

17 anions. (b) UV−vis titration spectra of ONRs with 2 equiv. of Al^{3+} upon addition of
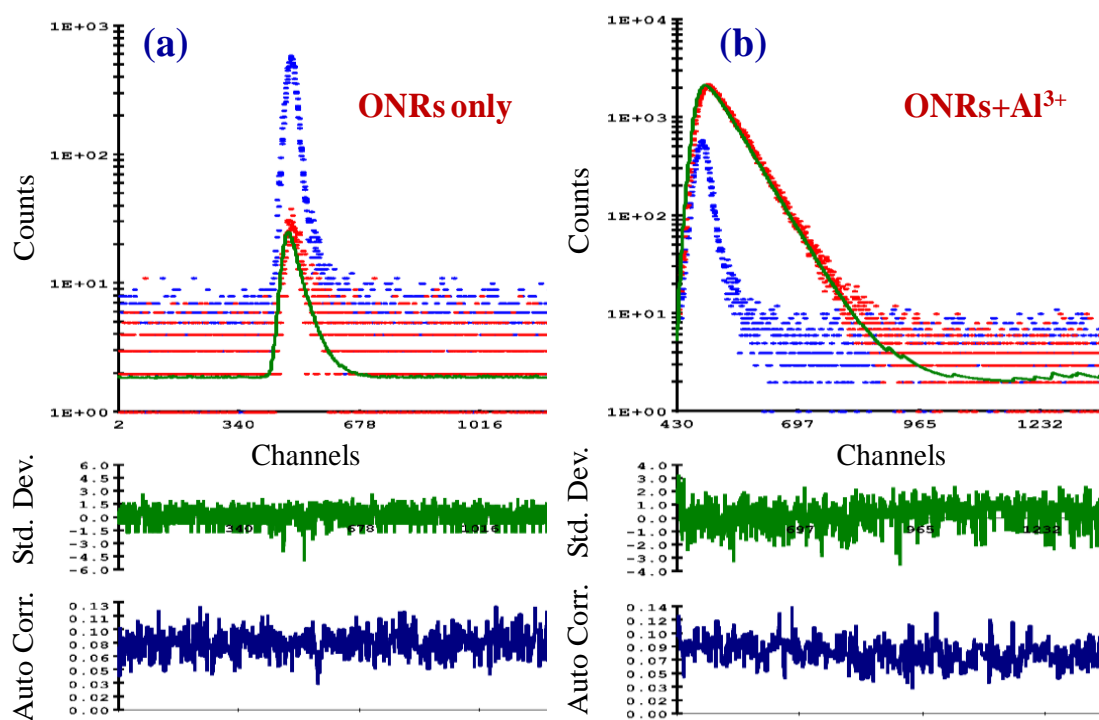
18 sodium sulfide (30 μM) in aqueous solution.

1

2

3

4

5

6

7

8

9

10

11

12   **Figure 7.** (a) Changes in the fluorescence spectra of ONRs−Al^{3+} complex in presence of

13   different anions. (b) Fluorescence titration spectra of ONRs with 2 equiv. of Al^{3+}

14   upon addition of sodium sulfide (30 µM) in aqueous solution.
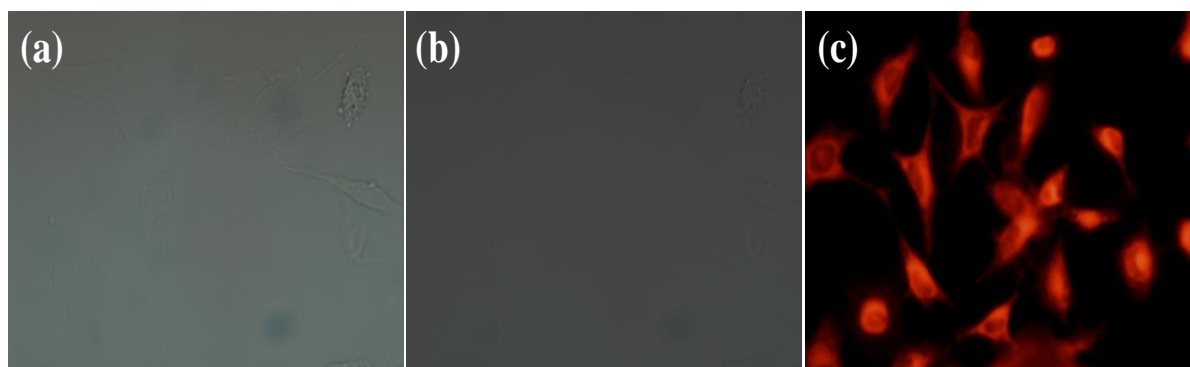
15

1

2

3

4

5

6

7

8

9

10

11

12

13

14

15

16

17

18

19

20

21

22

23

24

25

26

27

28

29 **Figure 8.** Lifetime measurement studies of ONRs (a) and ONRs–Al^{3+} (b).

31

1

2

3

4

5

6

7

8

9

10

11

12

13

14 **Figure 9.** The fluorescence microscope images of HeLa cells with absence of metal ions ONRs

15 (a), Al^{3+} (b) did not show any fluorescence and ONRs-Al^{3+} (c) showed intense red

16 fluorescence.

1

2

3

4

5

6

7

8 **Biographies**

M. Maniyazagan received his M.Sc. degree in organic chemistry from Muthayammal college of Arts and Science, Periyar University, India in 2008. He is currently a Ph. D candidate working in synthesis of rhodamine based derivatives and fluorescent sensor materials under the guidance of 13 Dr. T. Stalin at Department of Industrial Chemistry, Alagappa University, Karaikudi, India

R. Mariadasse received his M.Sc. degree from Pondicherry University in 2013. Currently he is working as a Ph.D. Research Scholar under the guidance of Dr. J. Jeyakanthan at Department of Bioinformatics, Alagappa University, Karaikudi, Tamil Nadu, India. His research interests focus on 18 the Computer Aided Drug Design.

M. Nachiappan, I am graduated with master degree in the branch of Bioinformatics and as I am fascinated on the structural biology research; I have opted the small molecules to study the nature, structure and their important roles in the biological system.

23

Gandhi Sivaraman received his B.sc., (Chemistry) from Thiyagarajar college (Madurai Kamaraj University) in 2007, M.sc., (Chemistry) from The American college (Madurai Kamaraj University) in 2009. He received his Ph.D from the same university under the guidance of Prof. D. Chellappa in 2014. He is currently working as a bridging fellow in institute of stem cell biology and regenerative medicine (instem), Bangalore, India. His research interests are Chemosensors, Chemical Biology, and Computational Chemistry.

P. Muthuraja has obtained his Master Degree in Chemistry in 2008 and now is pursuing for his Doctoral degree under the guidance of Dr. P. Manisankar at Department of Industrial Chemistry, Alagappa University, Karaikudi, India.

Dr. S. Naveen obtained MSc and PhD in Physics from the University of Mysore, Mysore. Presently he is working as a Scientist at The Institution of Excellence, University of Mysore, India. He was a Centenary Postdoctoral fellow at the Molecular Biophysics Unit, Indian Institute of Science, Bangalore. Dr. Naveen has published more than 150 articles in highly reputed International journals and is a member of many professional bodies.

Dr. N. K. Lokanath obtained PhD in Physics from the University of Mysore, Mysore. Presently he is working as a Professor at Dept. of Studies in Physics, University of Mysore, India. Recently, he was awarded the Sir C V. Raman Young Scientist's State Award from Government of Karnataka for his outstanding contribution towards science. Prof. Lokanath's area of research includes structural biology and new materials. He solved the first crystal structure of A-ATPase from *Pyrococcus horikoshii* which was acclaimed worldwide as a significant

finding. He has determined structures of more than 75 proteins and has published more than 150 articles.

Dr. J. Jeyakanthan, Professor and Head in the Department of Bioinformatics, Alagappa University, Karaikudi. He has published 83 research articles in the reputed National and International journals and more than 100 Protein crystal structures depositions in Protein Data Bank (PDB). He has received Rs. 2.21 cores funds from various agencies such as UGC, DBT, and DST and being the Coordinator of UGC Sponsored Innovative Scheme in the department. He is visiting scientist of Osaka University and RIKEN Spring-8 Institute, Japan. Currently, 8 scholars are doing Ph.D under his guidance. He has visited many countries.

Dr. P. Manisankar is currently Professor and Head, Department of Industrial Chemistry, Alagappa University, Karaikudi, Tamil Nadu, India. He obtained his M.Sc. from V.O.C. College, Tuticorin and Ph.D. from Madurai Kamaraj University, Madurai. His current research area of interest includes conducting polymer composites, sensors, dye sensitized solar cells, green synthesis of organic compounds. He has generated funds to the tune of Rs.400 lakhs. He is a recipient of TANSA 2009 award from Tamil Nadu State Council for Science and Technology and UGC BSR one time grant award. He has produced 30 Ph. D scholars and published 172 papers in the referred journals.

Dr. T. Stalin is an Assistant Professor of Chemistry in the Department of Industrial Chemistry at Alagappa University, Tamilnadu, India. He received his Ph. D degree from Annamalai University, India. He is a recipient of DST-Fast Track Young Scientist Award from Indian

5   Government and received prestigious award of Raman Fellowship from

6   UGC for Post-Doctoral Research in USA to have international collaborative research

7   opportunities to advance his research skills in emerging field. His current research interest

8   involves the development of chemo-sensor materials for environmental and biological

9   applications. He has generated funds of Rs.60 lakhs for his research. He has supervised 7   Ph.

10 D scholars and published more than 45 highly reputed research articles in science citation index

11 journals. He is a Life member of the Indian science congress Association, Solid State

12 Chemistry.

13

14